Development of a new mixing rheometer for studying rheological behaviour of concentrated energetic suspensions

Jean-Philippe Guillemin, Yves Ménard, Luc Brunet, Olivier Bonnefoy, Gérard Thomas

Development of a new mixing rheometer for studying rheological behaviour of concentrated energetic suspensions

J.P. Guillemin[a,*], Y. Menard[a], L. Brunet[a], O. Bonnefoy[b], G. Thomas[b]

[a]*Nexter Muntions, Engineering Direction, 7 route de Guerry, 18023 Bourges Cedex (France)*
[b]*Ecole Nationale Supérieure des Mines de Saint-Étienne, Centre SPIN/LPMG, UMR CNRS 5148, 158 Cours Fauriel, 42023 Saint-Étienne Cedex 2 (France)*

Abstract

The overall objective is to present a procedure based on a Couette analogy to quantitatively analyse torque/rotor speed data and extract viscosity/ shear-rate curves using a non-conventional geometry. Diphasic flows of energetic concentrated suspensions of melt-cast insensitive explosives exhibit particular rheological properties. The characterization of these complex fluids may be a challenging task when conventional rheometers are used. Placing these dense suspensions in a classic cylindrical geometry may lead to a partial destruction of the internal fluid structure. To prevent that, a "RheoXF" a mixer-type rheometer has been developed: it consists in a mixing device with quite a complex geometry rotating in a cylindrical tank. To evaluate the rheological constants (virtual radius, virtual shear rate and stress constants) of thus mixing rheometer, we used five Newtonian fluids. After this calibration, the rheological characterizations were carried out on five formulations. The unique parameter which changes in these formulations is the batch's origin of a secondary explosive: the 3-nitro-1,2,4-triazole-5-one . These energetic particles differ by their morphology, maximum packing density and may be by their process synthesis. After having determined pseudoplastic parameters, a correlation has been made with the evolution of maximum packing density values calculated with De Larrard model.

Keywords: Couette analogy, Mixer-Type rheometry, Complex fluid, Pseudoplastic parameters, De Larrard model

1 Introduction

Special series of formulations (XF13333) used in the ammunition 155 LU-211-M have been considered to elaborate explosives implemented by melt cast process. The formulation must satisfy one first primary criterion: an industrially profitable cast time.

Fig. 1. LU-211-M (on the left) and the melt cast process (on the right)

The XF13333 formulation is composed of a liquid phase made up of 2,4,6-trinitrotoluene, wax and surfactant and a solid phase composed of 3-nitro-1,2,4-triazol-5-one and aluminium (the solid volume fraction is higher than 0.50). The granular species have an average particle size of 200-600 µm for 3-nitro-1,2,4-triazol-5-one and 10-30 µm for aluminium.

*Corresponding author: jp.guillemin@nexter-group.fr / jp.guillemin@gmail.com

For highly concentrated suspensions, the viscosity has a strong, non linear, dependence with particle interactions. Beyond a certain solid volume fraction, the viscosity of suspensions increases more and more strongly as the solid loading level increases, until one reaches the maximum packing density ϕ_m . A recent study has shown that the melt-cast explosive flow time principally depends on ϕ_m [1].

This complex fluid cannot be characterized by a single measurement of viscosity in a rheometer with traditional geometry. In rheometry, the use of several mixing impellers makes it possible to characterize the fluid flow over a broad range of rheological properties [2-3-4]. Typical rotational rheometers include coaxial cylinders, cone and plate and parallel plate rheometers. Each geometry has obviously its advantages but also its drawbacks for a given fluid to characterize [5]. Rheological characterization of complex fluids such as XF13333 might be a challenging task when conventional rheometers are used. Placing this energetic concentrated material in such geometries may result in a partial destruction of the internal structure (caused by phase separation, sedimentation or flotation which may occur in a short timespan, between 1 and 10 min), and thus distort the rheological characterization.

To overcome this problem, a new mixing impeller, RheoXF has been designed, and mounted on a conventional rheometer. Its key features are:

- low required energy levels (risk of destabilisation)
- good mixing ability (keep the formulation homogeneous)
- small size (adaptable to standard Couette rheometers)

The viscosity, shear rate and shear stress are deduced from the speed and the torque measurements.

In this work, a new procedure based on Couette analogy will be proposed to quantitatively analyse torque/rotor speed data. In order to determine the stress constant and the shear rate constant, five experiments performed with model fluids. Then the rheological parameters, of each energetic suspension obeying the pseudoplastic model (power law or Ostwald model) are determined and correlated with the maximum packing density values calculated with a polydisperse packing model.

Nomenclature

A	torque/speed constant (N.m.s)
a_{ij}	wall effect exerted by the coarser particles
b_{ij}	loosening effect exerted by the finer particles
C	experimental packing density
H	distance from fluid free surface to the mixing-impeller (m)

k	consistency index (Pa.s^n)
$K_{\dot{\gamma}_v}$	virtual shear rate constant
K_τ	stress constant (Pa.N^{-1}.m^{-1})
M	torque (N.m)>0
n	flow index
N	rotational velocity (s^{-1})
r	variable radius (m)
R_{out}	radius of the cylindrical tank (m)
R_{in}	radius of the equivalent inner cylinder (m)
v_θ	tangential velocity (m.s^{-1})

Greek letters

α_i	volume fraction of particles belonging to class i
β_i	residual packing density *i.e.* when the class i is alone and fully packed
$\dot{\gamma}$	shear rate (s^{-1})
$\dot{\gamma}_v$	virtual shear rate (s^{-1})
η	suspension viscosity (Pa.s)
η_0	Newtonian viscosity of interstitial fluid (Pa.s)
ϕ	solid volume fraction
ϕ_i	packing density of class i
ϕ_m	maximum packing density
ρ_b	bulk density (g.cm^{-3})
ρ_t	true density (g.cm^{-3})
τ	shear stress (Pa)

2 Theories

2.1 Couette analogy

2.1.1 Determination of the virtual shear rate expression

First let us remember that a Couette rheometer is typically composed of two coaxial cylinders, which radius are very close from each other ($0<R_{out}-R_{in}<<R_{in}$). The gap between the two cylinders is filled with the fluid of unknown viscosity and the inner cylinder is rotating, while the outer one is kept motionless. Provided that the shear flow satisfies some characteristics, the measurement of the torque and rotation speed gives access to the fluid dynamic viscosity.

When the flow in a cylindrical tank (R_{out}) is established by a more or less standard impeller instead of a rotating inner cylinder, the Couette analogy [6-7] consists in determining the internal radius R_{in} for an equivalent virtual Couette system (the height H and outer radius R_{out} are kept constant).

The assumptions made on the laminar flow of an incompressible fluid in Couette geometry are as follows. The free surface flow remains horizontal. The disturbing effects related to the normal stress are thus negligible. This implies that the vertical velocity component is null. The flow effects at the bottom of the tank are negligible and the fluid slips perfectly along the horizontal surface of the virtual cylinder. The fluid is homogenous and the inertial effects are negligible. Under these conditions and in a virtual cylindrical referential, the system symmetry imposes that the only not-null component is the tangential velocity v_θ. The shear rate $\dot{\gamma}$ is thus given by:

$$\dot{\gamma} = r\frac{d}{dr}\left(\frac{v_\theta}{r}\right) \tag{1}$$

In cylindrical geometry, the general expression of the shear stress τ is given by:

$$\forall r, \quad \tau = -\frac{M}{2\pi H}.\frac{1}{r^2} \tag{2}$$

where M is the generated torque .

To establish a relation between shear stress and shear rate, an *a priori* assumption on the rheological behaviour of the fluid must be chosen. From previous work [8], we know that the XF13333 formulations give non-Newtonian systems and are quite well described by a pseudoplastic power law. So, we shall focus on fluids that obey the law:

$$\tau = k\dot{\gamma}^n \tag{3}$$

where k and n are the consistency and flow indexes, respectively.

With Eq. (1), Eq. (2) and Eq. (3) and after integration between R_{out} and R_{in}, we obtain the general shear rate expression:

$$\dot{\gamma}(r) = \frac{\frac{4\pi N}{n}\left(\frac{R_{in}}{r}\right)^{2/n}}{\left[1-\left(\frac{R_{in}}{R_{out}}\right)^{2/n}\right]} \tag{4}$$

where N is the rotational velocity (s^{-1}).

Combining Eq. (1) and Eq. (4) when $r = R_{in}$ provides:

$$R_{in} = \frac{R_{out}}{\left(1+\frac{4\pi N}{n}\left(\frac{2\pi k H R_{out}^2}{M}\right)^{1/n}\right)^{n/2}} \tag{5}$$

with $n = 1$ and $k = \eta$, the relationship between torque M and rotational velocity N becomes:

$$M = A.N \tag{6}$$

$$\text{with } A = \frac{8\pi^2 H R_{out}^2 R_{in}^2}{R_{out}^2 - R_{in}^2}\eta \tag{7}$$

where A is dependant of the Newtonian fluid viscosity η. After having defined the internal radius of our virtual Couette geometry, we can define the virtual shearing rate $\dot{\gamma}_v$ given by:

$$\dot{\gamma}_v = \frac{v_\theta(R_{in})}{R_{out}-R_{in}} \tag{8}$$

Combining Eq. (1), Eq. (2), Eq. (3) and after integration between R_{in} and R_{out} gives:

$$v_\theta(R_{in}) = \frac{n}{2}\left(\frac{M}{2\pi H k}\right)^{1/n} R_{in}\left(R_{in}^{-2/n} - R_{out}^{-2/n}\right) \tag{9}$$

Finally $\dot{\gamma}_v$ can be calculated with Eq. (5), Eq. (8) and Eq. (9). The result corresponds to Eq. (10):

$$\dot{\gamma}_v = K_{\dot{\gamma}_v} .N \tag{10}$$

$$\text{with } K_{\dot{\gamma}_v} = \frac{2\pi R_{in}}{R_{out} - R_{in}} \tag{11}$$

Let us notice that $K_{\dot{\gamma}_v}$ is nothing else than the Metzner Otto constant, well-known in the field of agitation-mixing [9]. As we can see it and with the evoked assumptions, $K_{\dot{\gamma}_v}$ is independent of the behaviour of the fluid Newtonian or not. This result is experimentally observed by many authors [10-11-12-13]. Some Computational Fluid Dynamic approaches give the same result [14].

2.1.2 Determination of shear stress constant

Contrary to the virtual shear rate, the shear stress constant K_τ can be determined without the assumption of a virtual geometry. Indeed, the shear stress τ is macroscopically observable for any geometry. Thus τ can be directly given by the following expression:

$$\tau = K_\tau .M \tag{12}$$

Combining Eq. (3), Eq. (9) and Eq. (11), we find:

$$K_\tau = \frac{k.\left(K_{\dot{\gamma}_v} .N\right)^n}{M} \tag{13}$$

This constant can be determined for Newtonian fluids (with $n = 1$ and $k = \eta$)

2.2 Relations between viscosity and the maximum packing density

Since the publication of Einstein analysing the viscosity of dilute suspensions of rigid spheres in a viscous liquid, numerous equations have been proposed to try and extend Einstein's formula to suspensions of higher concentrations. For example, three rheological expressions are given in Tab. (1).

Table 1. Rheological equations uses un the field of concentrated suspensions

These relationships express the viscosity of dispersions of spherical particles as a function of the viscosity of the interstitial fluid η_0 , the volume fraction of solids ϕ and the maximum packing density of the solids ϕ_m. Thus for a constant volume fraction of solids, the viscosity relationships derive from the general expression:

$$\eta = \eta_0 \cdot \psi\left(\phi_m\right) \tag{14}$$

Where $\psi(\phi_m)$ represents a function of ϕ_m.

XF13333 formulations present a volumic solid fraction higher than 0.50. At this point, particle interactions can influence viscosity more and more strongly as the level of solids increases until reaches the maximum packing density ϕ_m . Many strong similarities appear between concrete and explosives like XF13333 (great number of granulometric scales, range of the component morphologies, …). A number of packing models have been developed over the past 70 years, such as Furnas [18], Aim [19], Toufar [20], Stovall [21], Devar [22], and the De Larrard models [23-24]. Reviews by both Johansen [25] and Dewar [26] concluded that Furnas and Aim models are unsuitable for concrete mix constituent proportioning and are, therefore not considered in this study. In this kind of approach, the model developed by De Larrard, in the field of concrete suspensions, seems very attractive [24]. This model predicts the maximum packing density of a polydisperse mix, from three parameters: the particle size distribution of the mix, its true density and the experimental packing density of the solid species. The use of software is required to determine the maximum packing density. In this study, the RENE-LCPC software developed by De Larrard and T. Sedran [27] has been selected. The details of the algorithm will not be described here but the interested reader may refer to some of the associated publications [21-28-29].

This model deals with grain mixtures in which linear combinations of packing densities allow to predict the packing density of a mixture of monosized particles d_i ($d_1<d_2<\ldots<d_n$) from:

$$\phi_i = \frac{\beta_i}{1-(1-\beta_i)\sum_{j=1}^{i-1} a_{ij}\alpha_i - \sum_{j=i+1}^{N} b_{ij}\alpha_j} \tag{15}$$

Where ϕ_i is the packing density of class i; α_i is the volume fraction of solid particles belonging to class i; β_i is the residual packing density *i.e.* when the class i is alone and fully packed. To compute the packing density of the overall mixture, one considers that the bulk volume of the class i fills the porous space around the coarser grains; moreover, the volume of finer classes inserted in the voids of class i must be added. Two interaction effects must be taken into account in this calculation: the wall effect, a_{ij}, exerted by the coarser particles and the loosening effect, b_{ij}, exerted by the finer particles. Finally, ϕ_m is given by Eq. (16).

$$\phi_m = \min_{1<i<N} \phi_i \tag{16}$$

3 Experimental Set-up, materials and protocol

3.1 Experimental set-up

Conventional Couette rheometers are not be used to perform viscosity measurements on XF13333 (due to phase separations, segregation, flocculation…). So, a home made rheometer, composed of a cylindrical tank and a specially designed impeller, has been developed. A shearing spindle, called RheoXF, is drawn on Fig. (2) using commercial Computer Aided Design (CAD) software Pro/Engineer.

Fig. 2. RheoXF CAD with Pro/Engineer

Fig. 3. Dimensions of new mixing-impeller (H = 17.70 mm, R_1 = 19 mm, R_2 = 14.26 mm, R_{out} = 24.05 mm, φ = 5°, θ = 15°)

To control the temperature (+/-0.1°C), a regulated bath (Haake) is used.

3.2 Rheometer calibration method

To calculate the virtual inner radius R_{in} defined above, three steps are necessary:

- measuring the dynamic viscosity of a given Newtonian fluid at 25°C with a conventional Couette rheometer (Rheomat 30, Contraves),
- measuring the torque-speed data when the same fluid is agitated in the home-made rheometer,
- use the Couette analogy to calculate the virtual inner radius R_{in}.

To improve the quality of the calibration, five Newtonian fluids: Liquiflex are considered. These fluids are hydroxyl terminated polybutadiene (Liquiflex H), Urethane H200-AT Vosschemie, Glycerol Prolabo 99.65%, Rhodorsil silicon oils 47V500 and 47V20.

3.3 XF13333 formulations

Five XF13333 formulations are studied. The compounds used in these formulations are listed in Tab. (2). Mass fractions are given in Tab. (3).

Table 2. Compounds used in XF13333 formulations

Table 3. Mass fractions of the different compounds used in XF13333 formulation.

We used five NTO samples, referred to as: E1, E2, E4, D and D'. These NTO exhibit approximately the same particle size distribution (150-800 µm). They differ by their morphology (Fig. (4)) and by their experimental packing density (Tab. (4)). Another difference between NTO samples can come from their process of synthesis but this information could not be obtained by the suppliers. Aluminium powder, ECKA MEP 163 CL RE 925 (noted Al) has an average size of 15 µm (Fig. (5)). The experimental packing density C is calculated from the true and bulk densities:

$$C = \frac{\rho_t}{\rho_b} \tag{17}$$

The true density ρ_t is measured with a helium pycnometer from Micromeritics (AccuPyc 1330) and the bulk density ρ_b with a volumenometer.

Fig. 4. NTO morphologies obtained by scanning electron microscopy. E1, E2 and E3 NTO particle shapes are less regular than D and D' NTO particle shapes.

Fig. 5. Aluminium morphologies obtained by scanning electron microscopy. Aluminium particle shapes are irregular.

Table 4. Bulk density ρ_r, True density ρ_t and experimental packing density C of granular species

3.4 Determination of pseudoplastic parameters

For each XF13333 formulation, the RheoXF mixer is used to obtain homogeneous concentrated suspensions. Each formulation is mixed at 350 rpm during 30 min at 85°C. Then, every 5 seconds, the rotational speed is decreased stepwise. For each step, that lasts 5 seconds, the torque is measured at a given rotational velocity.

4 Results and Discussions

4.1 Rheometer calibration

For determining the virtual inner radius, the virtual shear rate and the stress constant, rheological curves with a standard Couette rheometer has been determining at 25°C for five typical liquids. All fluids appear to be Newtonian. For each test fluid, the slope of the curve gives the dynamic viscosity and standard deviation as shown in Tab. (5).

Table 5. Viscosity η of Newtonian fluids obtained Couette geometry at 25°C

Then, the same five test-fluids are characterized with the new RheoXF rheometer. Measurements of the torque (M) for several values of the rotational speed N lead to the determination of slope values A. Finally, the relationship between A (given by RheoXF) and η (given by a Couette rheometer) allows the calculations of the virtual radius R_{in}, the virtual shear rate constant $K_{\dot{\gamma}_v}$ and the stress constant K_τ.

Fig. 6. Torque/Speed data for each Newtonian fluid characterized with RheoXF at 25°C

Table 6. A values for each Newtonian fluids at 25°C

Fig. 7. Correlation between A coefficient and viscosity η

Fig. 8. Correlation between torque M and shear stress τ. Curve slope gives the shear stress constant K_τ

The estimated R_{in}, $K_{\dot{\gamma}_v}$ and K_τ values for this non-conventional geometry are respectively 17.170±0,004 mm, 15.691±0.003 and $18.59.10^3$±$0.14.10^3$ $Pa.N^{-1}.m^{-1}$. The virtual shear rate constant (*i.e.* Metzner-Otto constant) is found to be of the same order of magnitude as those obtain with other complex geometries similar to RheoXF impeller design. For example, the Metzner-Otto constant is equal to 10 (resp. 11.58) for a marine propeller (resp. harness with six right blades) [9].

4.2 Rheological measurements of XF13333 formulations

The rheological behaviour of XF13333 formulations, obtained using RheoXF is shown on Fig. (9). Two formulations (E4 and D') are characterized using Couette

geometry. Rheological curves are given in Fig (10). As we can observe, the rheological curves using Couette Geometry give a rheological signature which doesn't correctly quantify the flow behaviour of these two suspensions.

Fig. 9. Rheological curves of XF13333 formulations, obtained using RheoXF, at 85°C

Fig. 10. Rheological curves of XF13333 at 85°C with Couette geometry.

The experimental curves, obtained using RheoXF, can be satisfactorily fitted with a power law as mentioned in Eq. (3). The corresponding pseudoplastic parameters *k* and *n* are given in Tab. (7). These coefficients are obtained by method of least squares on experimental curves.

Table 7. Consistency index *k* and flow index *n* of XF13333 formulations at 85°C.

4.3 Correlation with maximum packing density

The measured consistency index *k* and flow index *n* are plotted as a function of the reduced volume fraction ϕ/ϕ_m for each XF13333 formulation. As Fig. (11) shows, *k* decreases when the ratio ϕ/ϕ_m decreases. In other words, the lower *k*, the less viscous the energetic paste.

Fig. 11. Evolution of the consistency index *k* at 85°C with ϕ/ϕ_m where ϕ_m is calculated using De Larrard model

A correlation between the flow index *n* and ϕ/ϕ_m is also established. Fig. (12) shows an increase of *n* with a decrease of ϕ/ϕ_m. For a given ϕ_m value, we find the intuitive result that the fluid tends to behave as Newtonian ($n = 1$) when the solid volume fraction ϕ tends to zero.

Fig. 12. Evolution of flow index *n* at 85°C with ϕ/ϕ_m where ϕ_m is calculated using De Larrard model

5 Conclusions

In spite of the complex nature of XF13333 formulations, the new RheoXF rheometer can offer the most reliable rheological analysis. The original geometry designed to realize an homogeneous formulation directly in a classic rheometer, enable us to determine rheological signatures of our energetic concentrated suspensions.

The procedure initially developed by Bousmina and al. [6] made it possible to quantify the flow behaviour of our suspensions. Definition of a virtual shear rate constant in a Couette flow leads also to the rheological fluid independence for the Metzner-Otto constant literal expression.

With the Couette Analogy, XF13333 formulations can be simply characterized and pseudoplastic parameters *k*, *n* determined. These parameters have been correlated with the maximum packing density ϕ_m calculated with the De Larrard model, initially developed for highly concentrated concrete suspensions. It was found that the consistency index *k* increases when the ratio ϕ/ϕ_m decreases and, on the contrary, that a rise of the flow index *n* was observed with a decrease of ϕ/ϕ_m.

References

[1] J.P. Guillemin, A. Weckerle, L. Brunet, O. Bonnefoy, G. Thomas, Application d'un modèle de viscosité à la coulée d'explosifs: modélisation du temps de coulée, Rhéologie, 10, (2006), 40-48

[2] J.F. Tranchant, A. Poulin, P. Marchal, L. Choplin, How to measure the rheological behaviour and the take up by means of mascara brush in the container, XXIth IFSCC International Congress, Proceedings, Berlin, (2000)

[3] L. Choplin, Génie des procédés et des produits assisté par rhéologie, 40ème Colloque annuel du Groupe Français de Rhéologie, Nice, (2005)

[4] Rajeev K. Thakur, Ch. Vial, G. Djelveh, M. Labbafi, Mixing of complex fluids with flat-bladed impellers: effect of impeller geometry and highly shear-thinning behaviour, Chem. Eng. Process., 43, (2004), 1211-1222

[5] N. El Kissi, S. Nigen, F. Pignon, Glissement et rhéométrie, Rhéologie, 10, (2006), 13-39

[6] M. Bousmina, A, Ait-Kadi, J.B. Faisant, Determination of shear rate and viscosity from batch mixer data: theoretical and experimental results, J. Rheol. 43, (1999), 415-433

[7] A. Ait-Kadi, P. Marchal, L. Choplin, A.S. Chrissemant, M Bousmina, Quantitative analysis of mixer-type rheometers using the Couette Analogy, Can. J. Chem. Eng., 80, (2002), 1166

[8] J.P. Guillemin, L. Brunet, O. Bonnefoy, G. Thomas, A flow time for melt-cast insensitive explosive process, Propellants, Explosives, Pyrotechnics, 32, 3, (2007), 261-266

[9] A.B. Metzner, R.E. Otto, Agitation of non-Newtonian fluids, *AICh J.*, 1, (1957), 3-10

[10] Mitsuishi and N. Hirai, J. Chem. Eng. Japan, 2, (1969), 217

[11] Gluz, M. D., and Pavlushenko, L. S. J. Appl. Chem., U.S.S.R., 39, (1966), 2323

[12] S. Nagata, Mixing-Principles and application, Kodansha Ltd. Tokyo & John Wiley, New York, (1975)

[13] F. Rieger, V. Novak, Chem, Eng. Sci, 29, (1974), 2229

[14] Murthy Shekhar, S. Jayanti, Mixing of pseudoplastic fluids using helical ribbon impellers**,** AIChE *J*, 49, 11, (2003), 2768-2772

[15] .M. Krieger, T.J. Dougherty, A mechanism for non-Newtonien flow in suspensions of rigid spheres, *Trans. Soc. Rheol.*, *3*, (1959), 137

[16] D. Quemada, Rheology of Concentratred Disperse Systems and Minimum Energy Dissipation Principle, I : Viscosity-Concentration Relationship, *Rheol. Acta*, *16*, (1977), 82

[17] M. Mooney, The Viscosity of a Concentrated Suspension of Spherical Particles, *J. Colloid Sci.*, *6*, (1951), 162

[18] C.C. Furnas, Flow of gasses through beds of broken solids, Bureau of Mines Bulletin, (1929), 307

[19] R.B. Aim, P.L. Goff, Effet de paroi dans les empilements désordonnés de sphères et application à la porosité des mélanges binaries, Powder Technology, 1, (1967), 281-290

[20] W. Toufar, M. Born, E. Klose, Contribution of optimisation of components of different density in

polydispersed particles systems, in 'Freiberger Booklet A 558', (VEB Deutscher Verlag für Grundstoffindustrie, (1976), 29-44 (in german)
[21] T. Stovall, F. De Larrard, M. Buil, Linear packing density for grain mixtures, Powder Technology, 48, (1986), 1-12
[22] J.D. Devar, Ready-mixed concrete mix design, Municipal Engineering, 3, (1986)
[23] J.D. Devar, Ready-mixed concrete mix design, Municipal Engineering, 3, (1986)
[24] F. De Larrard, T. Sedran, Mixture-Proportioning of High-Performance Concrete, Cement and Concrete Research. *32*, (2002), 1699
[25] V. Johansen, P.J. Andersen, Particle packing and concrete properties, Materials Science of Concrete, 2, (American Ceramic Society, Inc., Westerville, Ohio, (1996), 111-147
[26] J.D. Dewar, Computer Modelling of Concrete Mixtures, (E & FN Spon), 1999
[27] T. Sedran, F. De Larrard, *René-LCPC, Un Logiciel pour Optimiser la Granularité des Matériaux de Génie Civil*, Note Technique N°194, (1994). Laboratoire des Ponts et Chaussées, France
[28] F. De Larrard, *Formulation et Propriétés des Bétons à très Hautes Performances*, Rapport des Laboratoires des Ponts et Chaussées N°149, (1967). Thèse de Doctorat de l'Ecole Nationale des Ponts et Chaussées, France
[29] F. De Larrard, A General model for the prediction of voids content in high performance concrete mix design, *CANMET/ACI Conference on Advances in Concrete Technology*, Athenes, (1992)


XF
01-LUL-00

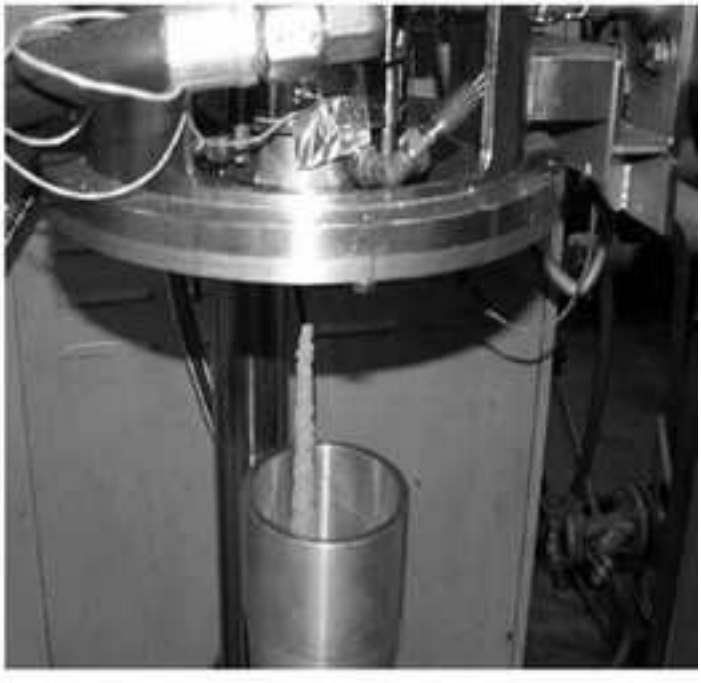

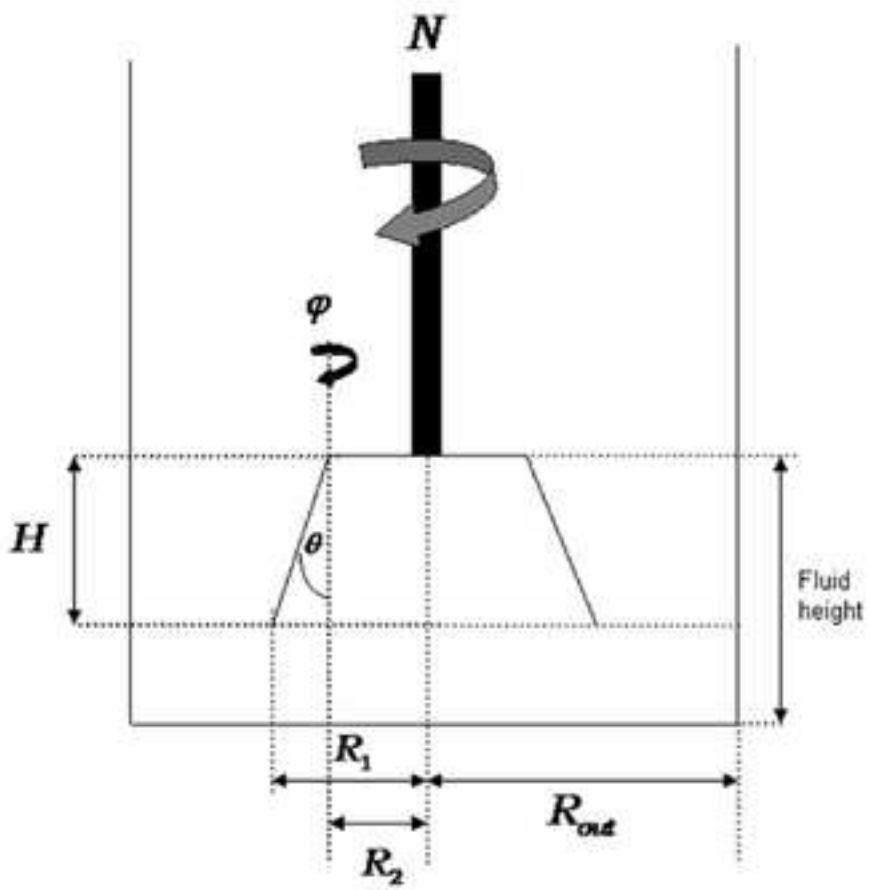
N
φ
H
θ
Fluid
height
R1
Rout
R2

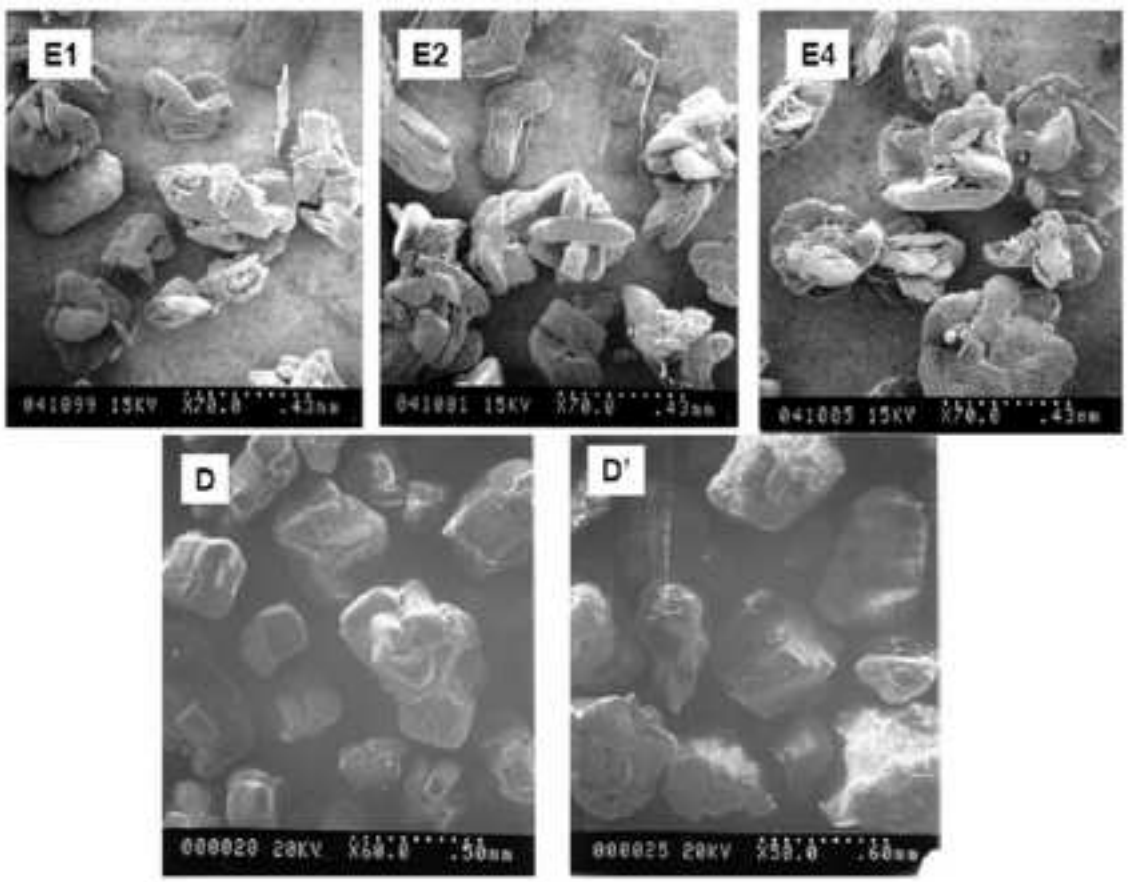
E1
E2
E4
D
D'

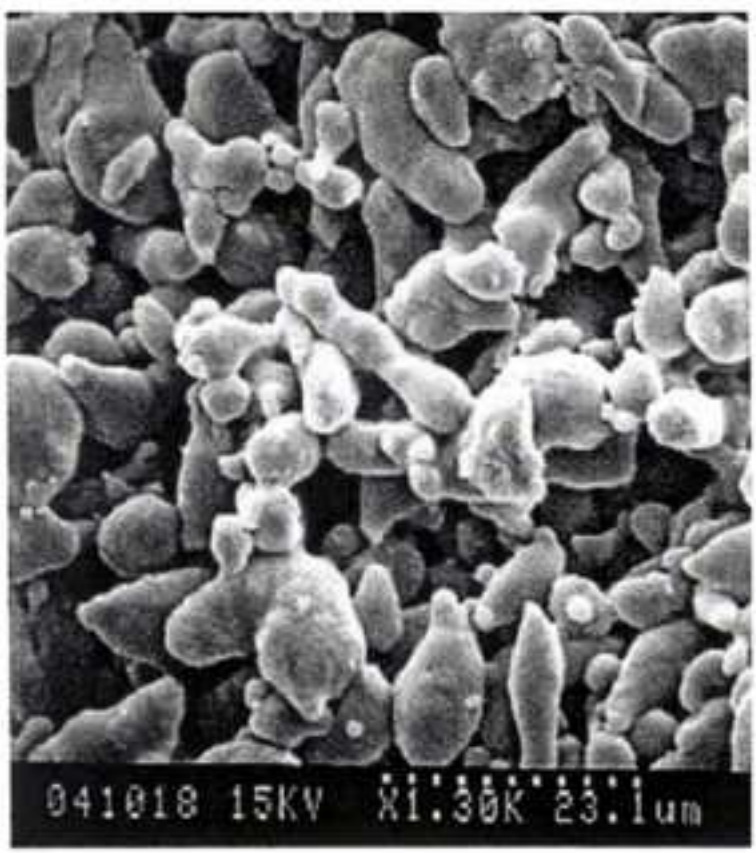
041018 15KV X1.30K 23.1um

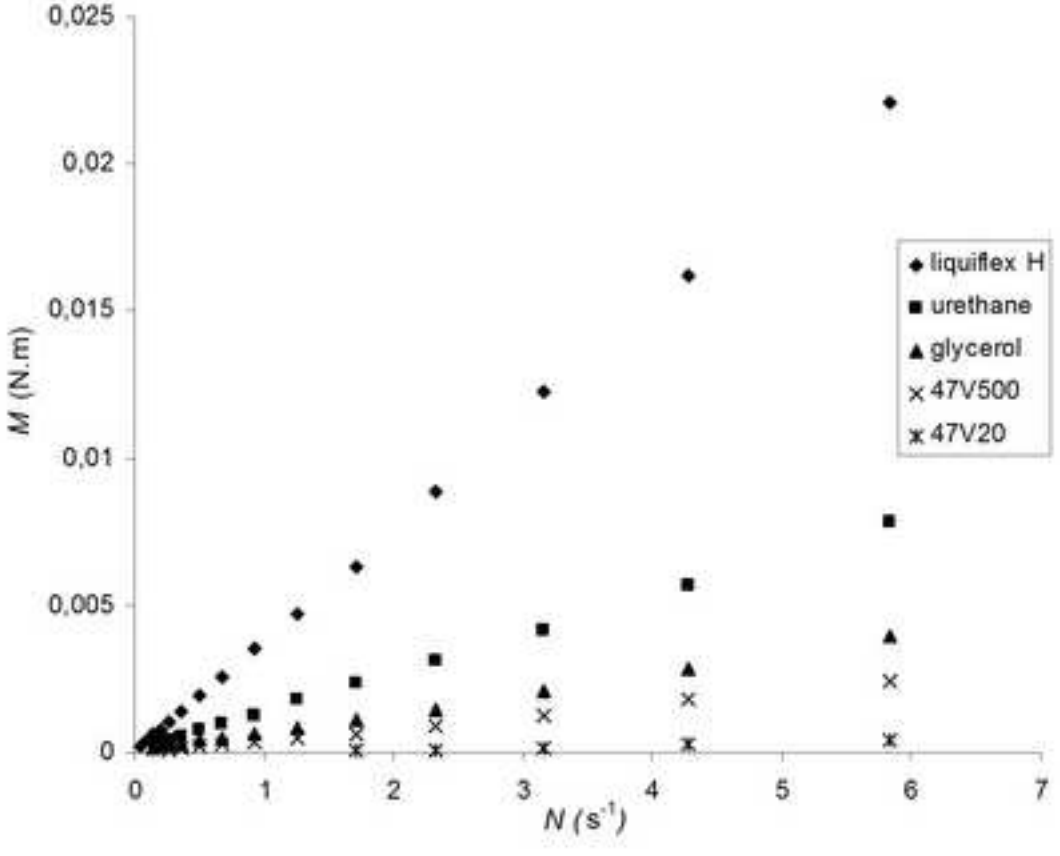
0,025
0,02
0,015
0,01
0,005
0
M (N.m)
0
1
2
3
4
5
6
7
N (s-1)
liquiflex H
urethane
glycerol
47V500
47V20

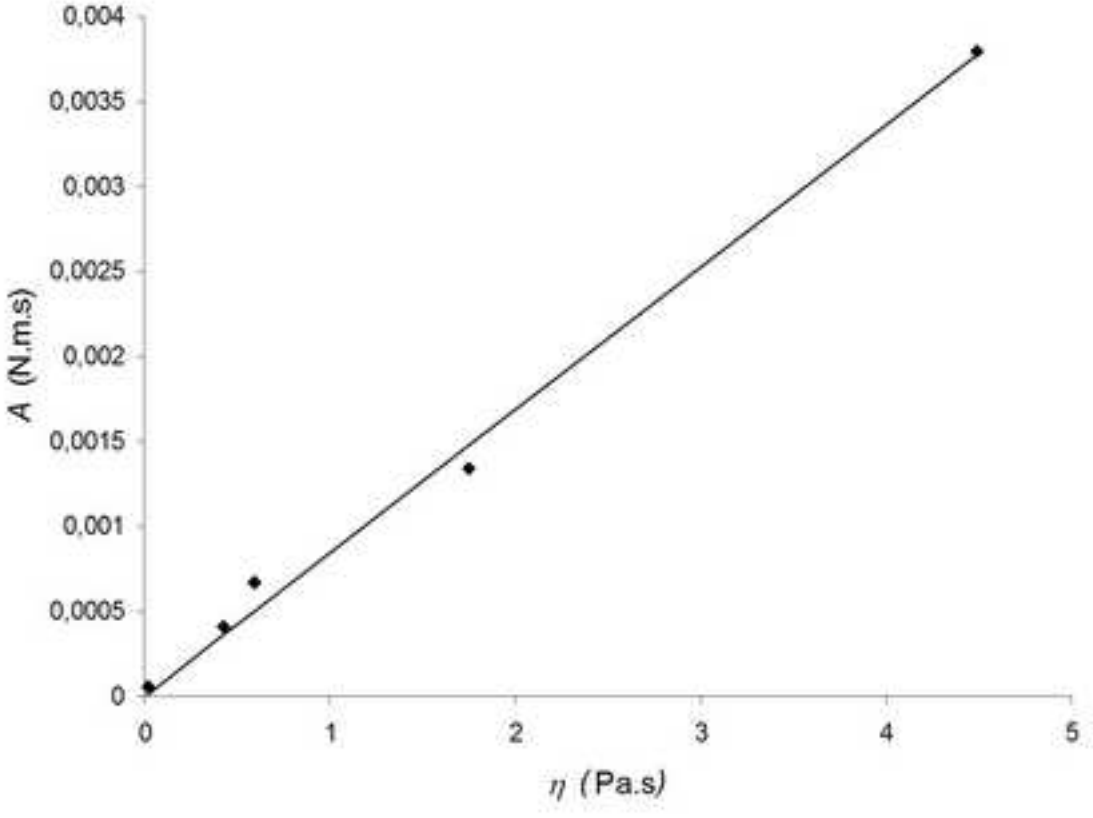
0,004
0,0035
0,003
0,0025
0,002
0,0015
0,001
0,0005
0
A (N.m.s)
0
1
2
3
4
5
η (Pa.s)

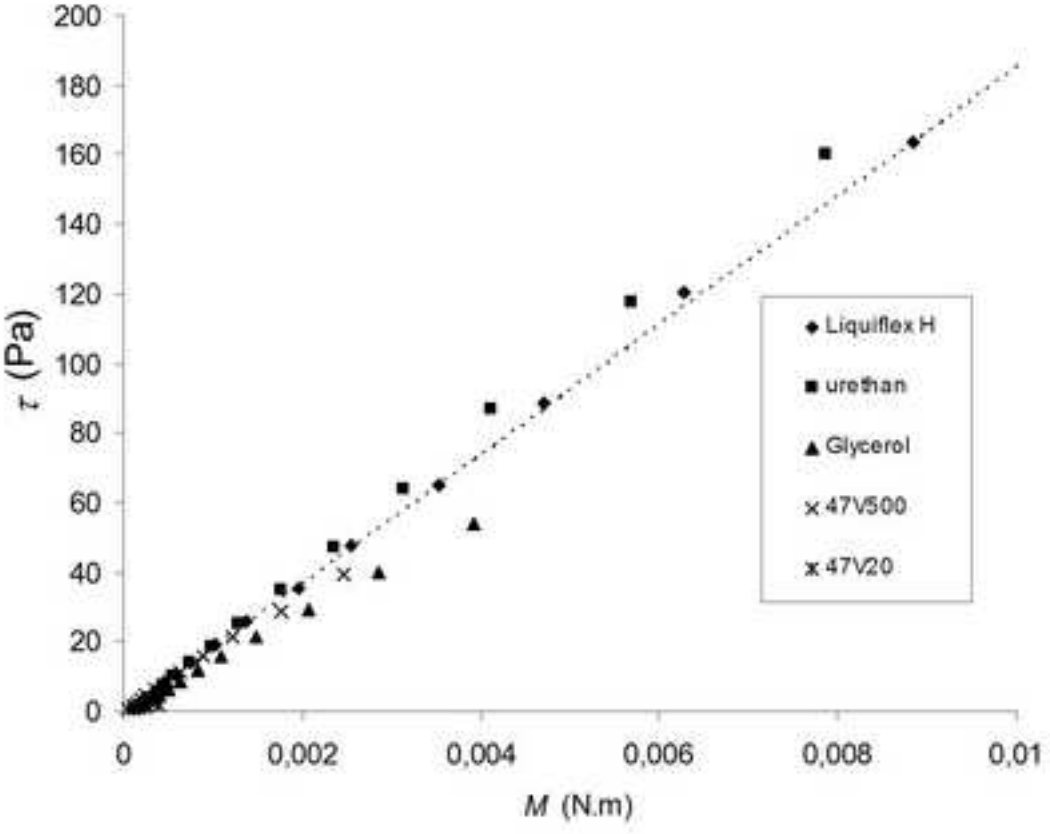
200
180
160
140
120
100
80
60
40
20
0
τ (Pa)
0
0,002
0,004
0,006
0,008
0,01
M (N.m)
Liquiflex H
urethan
Glycerol
47V500
47V20

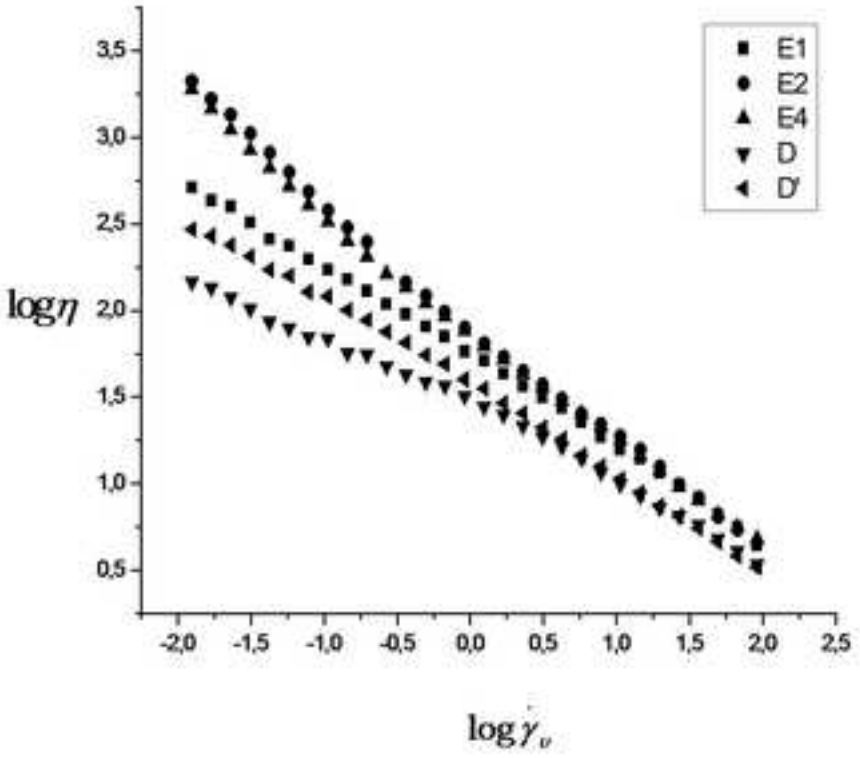
E1
E2
E4
D
D'
3,5
3,0
2,5
2,0
1,5
1,0
0,5
-2,0
-1,5
-1,0
-0,5
0,0
0,5
1,0
1,5
2,0
2,5
log η
log γ̇

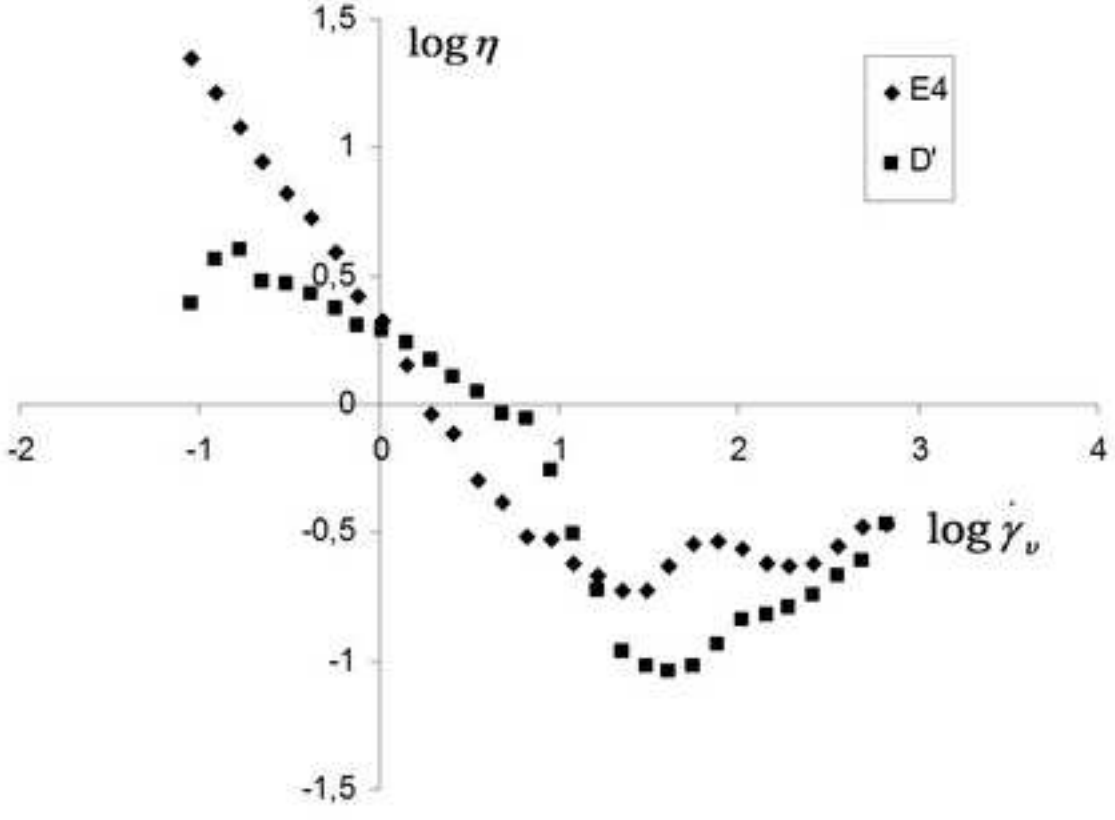
1,5
log η
1
0,5
0
-0,5
-1
-1,5
-2
-1
0
1
2
3
4
log γ̇ν
E4
D'

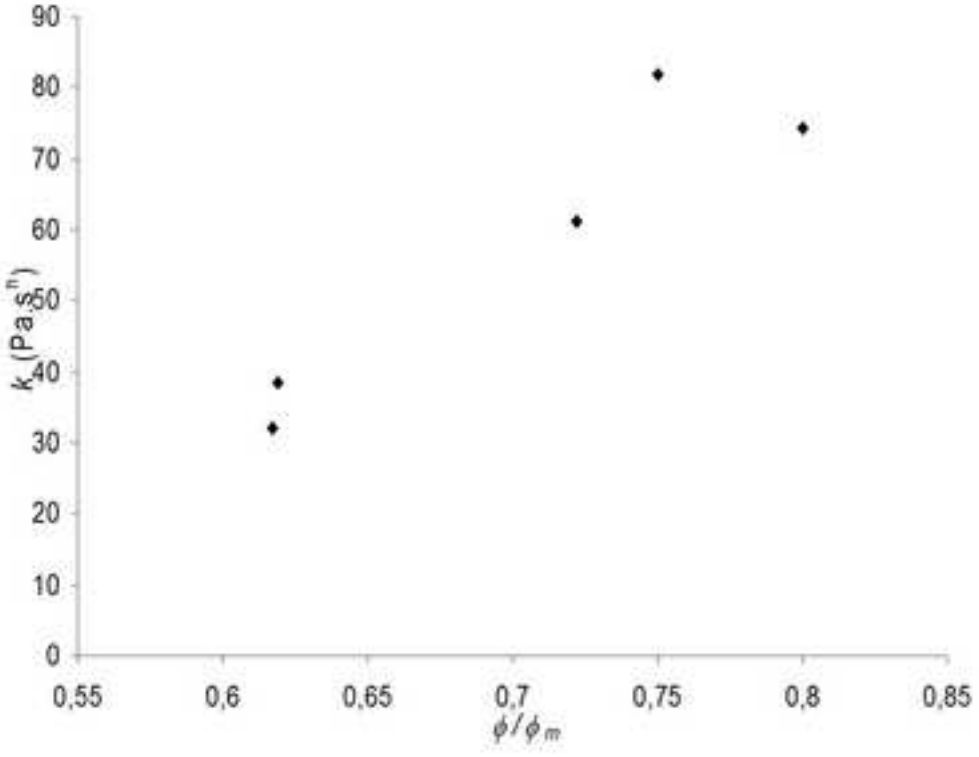
90
80
70
60
50
40
30
20
10
0
0,55
0,6
0,65
0,7
0,75
0,8
0,85
k_c (Pa.s^n)
ϕ / ϕ_m

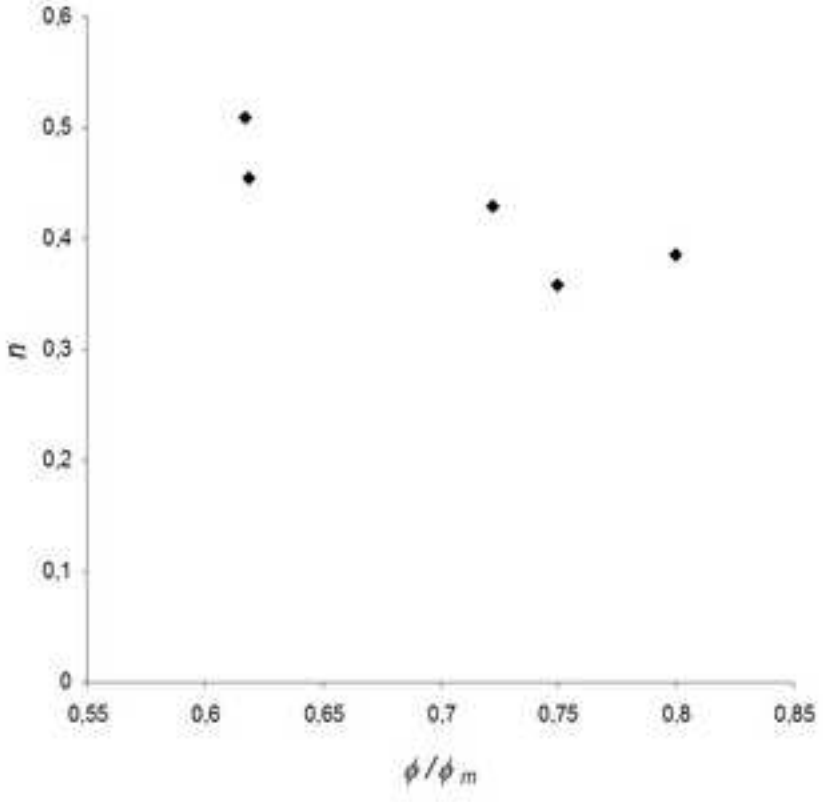
0,6
0,5
0,4
0,3
0,2
0,1
0
n
0,55
0,6
0,65
0,7
0,75
0,8
0,85
ϕ / ϕ m

Authors	Rheological Equations
Krieger – Dougherty [15]	$\eta = \eta_0 \left(1 - \frac{\phi}{\phi_m}\right)^{-2.5\phi_m}$
Quemada [16]	$\eta = \eta_0 \left(1 - \frac{\phi}{\phi_m}\right)^{-2}$
Mooney [17]	$\eta = \eta_0 \exp\left(\frac{2.5\phi}{1 - \frac{\phi}{\phi_m}}\right)$

	Name	True Density (g/cm^3)	Melting Point (°C)	Physical state at exp. Conditions
TNT	2,4,6-trinitrotoluene	1.65	81	liquid
A	Additive	1	83	liquid
Al	Aluminium	2.7	660	solid
NTO	3-nitro-1,2,4-triazol-5-one	1.92	279	solid

Compounds	Mass fraction w
TNT	0.310
A	0.075
Al	0.135
NTO	0.480

Raw Materials	ρ_r (g/cm^3)	ρ_b (g/cm^3)	C
E1	1.930	0.750	0.388
E2	1.926	0.790	0.412
E4	1.931	0.830	0.432
D	1.903	0.990	0.522
D'	1.889	0.970	0.515
Al	2.700	1.100	0.407

Newtonian fluid	η (Pa.s)	$\Delta\eta$ (Pa.s)
Liquiflex	4.4890	0.0110
Urethan	1.7518	0.0040
Glycerol	0.5909	0.0021
47V500	0.4263	0.0005
47V20	0.0197	0.0003

Newtonian fluid	A (N.m.s)	ΔA (N.m.s)	R^2
liquiflex H	0.003800	0.000011	0.99989
urethane	0.001340	0.000008	0.99978
glycerol	0.000670	0.000006	0.99929
47V500	0.000410	0.000005	0.99896
47V20	0.000060	0.000005	0.99682

NTO	k (Pa.s^n)	n	Δk (Pa.s^n)	Δn	R^2
E1	61.2	0.429	1.6	0.007	0.996
E2	82.0	0.358	1.8	0.006	0.996
E4	74.3	0.386	1.3	0.005	0.998
D	38.4	0.455	0.4	0.003	0.999
D'	32.0	0.509	0.7	0.006	0.998